View Article Online / Journal Homepage / Table of Contents for this issue

Mean-field models of structure and dispersion of polymer-nanoparticle mixtures

Venkat Ganesan,* Christopher J. Ellison and Victor Pryamitsyn

Received 22nd December 2009, Accepted 4th March 2010
DOI: 10.1039/b926992d

Published on 12 May 2010. Downloaded by University of Texas Libraries on 16/08/2013 15:20:49.

We review some recent research developments in coarse-grained modeling based on mean-field approaches of the equilibrium dispersion and structure of polymer nanoparticle composites. We focus on three issues: (i) dispersion and phase behavior of particles in homopolymer matrices; (ii) dispersion in mixtures of homopolymers with grafted nanoparticles; (iii) self-assembly and organization of nanoparticles in block copolymer matrices. In each of these topics, we highlight that the dispersability and the resulting structure of the nanoparticle suspension may exhibit far more complexities than one may deduce using simple miscibility criterion involving the energetic interactions between the polymer matrix and the particle. In each case, we review our own research contributions accompanied by a brief discussion of related theoretical studies and some possible future directions.

I. Introduction

Reinforcement of polymers using organic and inorganic particles (fillers) has become extremely common in a variety of practically important applications. Traditional applications in this context belonged to the "colloid" or the "composite" regime, where the filler size was typically larger than the size of the polymer. Not surprisingly, the composite limit has also had many advances in theoretical models and simulation approaches for predicting the equilibrium and dynamical properties of such mixtures.[1] However, more recent developments in nanotechnology applications have involved polymer-filler mixtures in the "nanoparticle limit" where the size of the polymer is comparable to or larger than one or more dimensions of the filler.[2–10] In such materials, termed polymer nanocomposites (PNCs), uniform dispersion of the filler particles results in significant interfacial contact between the polymer and the filler, which in many cases leads to new and novel properties arising from the unique synergism between materials.

Many researchers have demonstrated the potential of PNCs for a variety of applications.[4,5,10,11] For example, incorporating nanoscale dispersions of layered clay platelets, carbon nanotubes and nanosized silica particles into polymers has been shown to enhance both the amorphous and the rubbery modulii of the bare polymer matrix by as much as an order of magnitude.[2,3,12–14] Gas barrier properties of butyl rubber latexes was shown to be reduced by almost 2 orders of magnitude upon incorporating just 10 wt% of vermiculite fillers.[15] Addition of only 5% by weight of clay platelets were shown to reduce the fire hazard of nylon-6

Department of Chemical Engineering, University of Texas at Austin, Austin, TX 78712, USA

Venkat Ganesan

Venkat Ganesan is an Associate Professor and holds the Frank Liddell Centennial Fellowship in the Department of Chemical Engineering at the University of Texas at Austin. Venkat Ganesan's research interests center on the development of models, and simulation approaches for predicting the equilibrium and dynamical properties of multicomponent polymeric materials and polymer nanocomposites, and elucidating the structure-property, relationships in polymers used for fuel cell and organic photovoltaic applications. He was a recipient of an Alfred P. Sloan Fellowship (2004), a National Science Foundation's CAREER award (2004), a recipient of the American Physical Society's John H. Dillon Medal (2009) and a Kavli Fellow (2009).

Christopher J. Ellison

Christopher J. Ellison is an assistant professor in the Department of Chemical Engineering at the University of Texas at Austin. He conducted postdoctoral research from 2006–2008 in the Department of Chemical Engineering and Materials Science at the University of Minnesota after receiving his Ph.D. in chemical engineering from Northwestern University in 2005. His current research interests include synthesis and self-assembly of functional block copolymers, dynamics of nanoconfined polymers and hierarchical nanostructured polymers.

 This journal is © The Royal Society of Chemistry 2010

Published on 12 May 2010. Downloaded by University of Texas Libraries on 16/08/2013 15:20:49.

polymer by around 60%.[16,17] Similarly, polydimethylsiloxane (PDMS) filled with around 10% by weight of clay platelets displayed a 140 °C higher decomposition temperature compared to the pristine PDMS elastomer.[16] Mixtures of polymers with carbon nanotubes, semiconducting particles and magnetic particles have been demonstrated to possess novel electrical, optical and magnetic properties.[7,18–23]

Development and application of nanoscale multicomponent materials such as PNCs confronts a huge parameter space involving an interplay of constituent selection, fabrication, processing and performance.[11] In this article, we specifically focus on an issue which has commanded significant attention in PNCs, *viz*., *dispersion control of nanoparticles in polymer matrices*. Most combinations of polymers and pristine nanofillers tend to be immiscible, with the fillers undergoing aggregation either due to strong Van der Waals interactions between themselves or due to polymer-mediated interparticle attractions[5,6,3,9,24–26] (an example illustrating the dispersion issue is displayed in Fig. 1 [27]). Filler aggregation usually has a catastrophic effect on the properties of PNCs, since many characteristics of interest in PNCs typically depend on the significant interfacial area afforded at the nanoscale — a feature which is considerably eroded due to the aggregation of the fillers. Consequently, a significant issue confronting the development of PNCs for applications is to achieve well-dispersed filler configurations within the polymer matrix.

A simple understanding of the issues involved in the context of achieving particle miscibility and dispersability can be obtained by considering the surface tension of a spherical particle in a polymer melt displayed in Fig. 2. It can be seen that for cases where there are unfavorable interactions between the polymer melt and the particle, the surface tension is positive. One would expect that uniform dispersion of particles would not be favored in such situations and that the particles would prefer to either aggregate or separate out of the matrix. In contrast, favorable polymer–particle interactions lead to a negative surface tension. In such cases, intimate mixing between the polymer and particles lead to a lower free energy and therefore might constitute conditions favoring dispersability of the particles.

A number of experimental efforts have used the above guiding principles, and have focused on controlling the state of dispersion of nanofillers by a combination of one or more of the following strategies: (i) choosing the polymer-filler combinations appropriately to take advantage of favorable polymer–filler interactions; (ii) by "functionalizing" the fillers or the polymer matrix with a variety of anionic or cationic oligomeric surfactants and grafted polymers to exploit favorable interactions between the functionalizing group and the polymer matrix;[3,9,30,25,26,31] and (iii) using external fields such as electric, magnetic or flow fields to disrupt the equilibrium (aggregated) state and maintain it in a nonequilibrium dispersed and/or aligned configuration.[32]

While there have been a number of experiments reported along the above lines, the outstanding issue facing the development of theories, models and computer simulations to aid the design of such strategies is the following: "for a specified

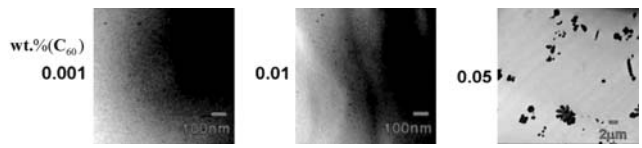

Fig. 1 (Adapted from ref. 27 with permission). TEM and optical micrographs of poly(methyl methacrylate) (PMMA)-C_{60} PNCs at different C_{60} wt%. The dark features are C_{60} agglomerates. At C_{60} wt% less than 0.01, C_{60} units are seen to be well-dispersed with agglomerate size units of scale around 20 nm in diameter. At C_{60} wt% = 0.01 nanoscale agglomerates are seen to coexist with micron sized agglomerates. For C_{60} wt% = 0.05, the C_{60} are seen to agglomerate into bundles of micron sizes.

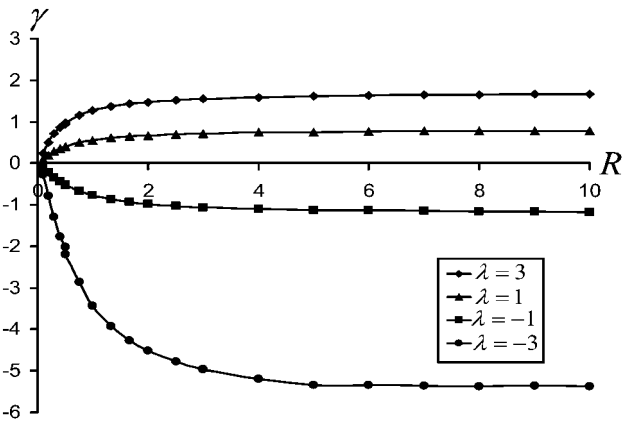

Fig. 2 Surface tension γ (in units nondimensionalized with k_BT/a^2, where k_B denotes the Boltzmann constant and a represents the Kuhn segment length of the polymer) between a particle of size R (in units nondimensionalized by the polymer radius of gyration) and a compressible polymer melt of flexible chains. The parameter λ (termed the adsorption length) quantifies the adsorption interaction between the polymer melt and the particle. Explicitly, $\lambda/a = \chi_s - \chi_{sc}$, where χ_s denotes the repulsion energy per monomer (in k_BT units) between the surface and the polymer. χ_{sc} denotes the critical interaction value between the polymer surface and the particle at which the adsorbed surface excess of the polymer is identically zero. Positive (negative) values of λ correlate to repulsive (attractive) interactions between the particle and the polymer. The polymer melt is modeled using a compressible polymer melt model described in ref. 28 with the nondimensional compressibility parameter chosen as 0.1. The interfacial tension was determined using the formalism described in ref. 29.

Victor Pryamitsyn

Victor A Pryamitsyn is a Research Associate in the Department of Chemical Engineering at the University of Texas at Austin. He received his Ph.D. in Physics of Polymers from the Institute of Macromolecular Compounds of Russian Academy of Sciences in 1987. His current research interests include theory and computer simulations of polymer and polymer nanocomposite materials.

View Article Online

Published on 12 May 2010. Downloaded by University of Texas Libraries on 16/08/2013 15:20:49.

combination of matrix polymer(s), filler(s) and the functionalizing moieties, can the expected structure and properties of PNC dispersions be predicted?" While the guiding principles discussed above have typically served as a good qualitative rule of thumb for choosing the different components, such simplistic principles suffer from several limitations. Explicitly, (i) such considerations do not account for the particle concentration effects as might be embodied within a detailed "phase diagram" for the polymer-particle mixture; (ii) the influence of size and chemical characteristics of the functionalizers (either small molecule or polymeric) is not accounted for; (iii) dispersion of particles in structured matrices such as the self-assembled phase of a block copolymer, cannot be gleaned from the above considerations.

Not surprisingly, overcoming the above limitations have constituted the focus of several recent theoretical investigations. Various methods, including computer simulations,[33–35] liquid state theories[36] and polymer field-theoretic approaches[37,38] have been used to address several aspects of the above issues. In our own research, we have adopted the use of coarse-grained modeling approaches to delineate the mechanistic features underlying the structure and dynamical properties of nanoparticle-polymer mixtures.[39–47] Such coarse-grained strategies typically involve the use of simple micromechanical models to represent the different components.[33,48–52] For instance, a common approach is to model the polymer as a connected sequence of segments, where each segment is understood to represent a collection of molecules or atoms.[50] Moreover, the polymer chain is typically (albeit, not necessarily) assumed to be fully flexible and behave as an elastic spring or a Gaussian coil. The particle fillers in such models may be represented as either hard spherical or anisotropic objects. Moreover, the different physicochemical interactions are represented by ignoring the specific chemical identities of the monomers and the resulting detailed interaction characteristics. Instead simpler model interaction potentials are used to characterize the interactions between segments of the polymer and the particle fillers. Such simplifying assumptions have enabled the implementation of analytical theories and/or long time and length scale simulations which allow one to discern the equilibrium[39,41,43,44,47] and nonequilibrium[45,46] structural characteristics of the nanofiller dispersion in polymer matrices. *We note that the main utility of such coarse-grained approaches lies in their ability to distill and characterize physical phenomena of interest in terms of a few macroscopic parameters*.

In this article, we review some of our recent contributions using such coarse-grained models and simulations to address the physical principles underlying the *equilibrium* aspects of dispersion strategies. Specifically, we focus on three issues: (i) dispersion and phase behavior of nanoparticles in homopolymer matrices;[39,41,43,44,47] (ii) dispersion in mixtures of homopolymers with grafted nanoparticles; (iii) self-assembly and organization of nanoparticles in block copolymer matrices.[42] Each of these topics serve to illustrate that the dispersability of nanoparticles may exhibit far more complexities than the simple miscibility trends one may deduce using the results of Fig. 2. Considering the breadth of this field and the rate at which new developments are reported, no attempt is made to render this a comprehensive review of each of the topics. Consequently, our review is very selective and focuses only on issues of our expertise and specifically on the developments which have arisen out of our own research. However, where appropriate, related theoretical and experimental studies and some possible future directions are briefly mentioned.

II. Phase behavior of nanoparticles in homopolymer matrices

The simplest model system pertinent to nanocomposite materials is that of a mixture of a homopolymer matrix (melt or solution) with nanoparticle fillers.[36] Whence, the first class of studies we review pertain to our contributions toward the modeling of the dispersion characteristics of spherical nanoparticle fillers in homopolymer solutions and melts. In this regard, we undertook several studies with an objective to obtain a fundamental understanding of the manner in which the polymer-polymer, polymer-filler and filler–filler interactions control the phase behavioral characteristics of such systems.[39,41,43,44,47] Specifically, our research was focused on understanding the influence of particle curvature and the specifics of the "nanoparticle limit" upon the overall phase behavior and particle structure in such polymer-nanoparticle mixtures.

That interesting curvature effects may manifest is clearly evident even from Fig. 2 where it is seen from the size dependence of the surface tension that the unfavorable or favorable mixing effects tend to be diminished for smaller sized particles. An outstanding question then is "are polymer-nanoparticle mixtures always miscible or is there a potential for richer phase behavior characteristics? "[53] To address this issue, our research has used coarse-grained polymer field theories[50,54] to address the dispersion characteristics of nanoparticles mixed with *polymer solutions*. Our approach was based on a rigorous formalism which integrates out the polymer "degrees of freedom" to derive polymer-mediated effective interaction potentials between the nanoparticles. Such interaction potentials were then combined with the bare particle–particle interactions within thermodynamic theories and/or computer simulations to shed light on the dispersion and structural characteristics of the nanoparticles in the polymer matrix. In the following, we first briefly outline the theoretical formalism we used and then subsequently discuss selected results from a few of our applications.

A. A mean-field approach to the phase behavior of polymer-nanoparticle mixtures

We developed a mean-field theoretic formalism to address the phase behavior of polymer-nanoparticle mixtures.[39,41] We adopted an implicit solvent framework comprised of a two component system of just particles (c) and polymers (p), interacting with each other by effective, solvent-averaged interaction potentials. Our formalism used a McMillan-Mayer like solution theory to formally recast the statistical mechanics of such a two-component system of polymer and particles into a *single* component system of just particles which interact by polymer-mediated effective interaction potentials in addition to their bare interparticle potentials. Explicitly, in a grand-canonical framework for the polymer solution, the polymer-mediated

 This journal is © The Royal Society of Chemistry 2010

Published on 12 May 2010. Downloaded by University of Texas Libraries on 16/08/2013 15:20:49.

pair-interaction potentials between nanoparticles $U(\mathbf{r}_i, \mathbf{r}_j)$ can be shown to be expressible as:[55,56]

$$U(\mathbf{r}_i, \mathbf{r}_j) = \ln \Xi_2(\mathbf{r}_i, \mathbf{r}_j; z_p, V) - \ln \Xi_1(\mathbf{r}_i; z_p, V) - \ln \Xi_1(\mathbf{r}_j; z_p, V) + \ln \Xi_0(z_p) \quad (1)$$

In the above equation, $\Xi_n(\mathbf{r}_i, \mathbf{r}_j, \ldots, \mathbf{r}_n; z_p)$ in general denotes the grand canonical partition function for the polymer solution at a fixed activity coefficient z_p containing n particles fixed at the positions $\mathbf{r}_i, \mathbf{r}_j \ldots \mathbf{r}_n$.

To obtain $\Xi_n(\mathbf{r}_i, \mathbf{r}_j, \ldots, \mathbf{r}_m; z_p)$ for the polymer solution, we implemented a mean-field theoretic approach commonly known as polymer self-consistent field theory (SCFT).[50,54] In a nutshell, polymer SCFT enumerates the statistical features and the thermodynamics of an interacting system of polymer chains by mapping them onto an equivalent system of noninteracting chains in the presence of pseudo chemical potential field(s), which in turn embody the interactions of a specified polymer chain with other polymer chains. The basis for such a formalism is established through field-theoretic techniques, which can be used to demonstrate that the thermodynamics of the system of noninteracting chains serves as a mean-field approximation to the thermodynamics of the system of interacting chains.[50] In a mean-field approximation, the intersegment interactions themselves are a function of the inhomogeneous densities of the appropriate components. The latter are in turn themselves influenced by the chemical potential field(s) acting on the polymer segments. Consequently, implementation of SCFT typically requires the self-consistent solution of a set of field equations for the chemical potential field(s).[50]

To implement the above formalism, we adopted a commonly used model for the polymers termed the Gaussian thread model.[57] In this model, the monomeric units of the polymers are assumed to be point-sized and the polymer chains themselves to be elastic threads connecting these monomers. The polymer–polymer interactions were modeled through effective excluded volume interactions which represent the combined effects of the polymer–polymer and polymer–solvent interactions.[50,57] In the SCFT formalism for polymer solutions, the effects of such excluded volume interactions are replaced by a spatially inhomogeneous chemical potential field, denoted as $W(\mathbf{r})$, which is determined as the solution of:

$$W(\mathbf{r}) = BC\phi\,(\mathbf{r}) \quad (2)$$

where B represents a nondimensional excluded volume parameter and C denotes the nondimensionalized overall polymer solution density. The field $\phi(\mathbf{r})$ represents the nondimensionalized inhomogeneous density field of the polymer segments. The above equation has a simple physical meaning in that it quantifies in a mean-field manner the excluded volume interactions experienced by a segment at location $\mathbf{r}$ due to the other intra and interchain polymer segments.

Eqn (2) is rendered a self-consistent condition by requiring that the density field $\phi(\mathbf{r})$ be itself obtained as a result of the statistics of the noninteracting chains in the external field $W(\mathbf{r})$. The main feature which allows for practical implementation of this formalism is the fact that the statistics of a polymer molecule in an external field can be determined by solving a diffusion equation for its distribution functions. For instance, for a polymer chain under the action of an external field $W(\mathbf{r})$, the probability $q(\mathbf{r}, s)$ that the sth segment of the chain lies at the position $\mathbf{r}$ (irrespective of the starting position of the chain) satisfies:[50,57]

$$\frac{\partial q}{\partial s} = \nabla^2 q - W(\mathbf{r}) q(\mathbf{r}, s); \quad q(\mathbf{r}, s = 0) = 1 \quad (3)$$

The density field $\phi\,(\mathbf{r})$ of the polymer can be expressed in terms of $q(\mathbf{r}, s)$ as:

$$\phi(\mathbf{r}) = \int_0^N ds\; q(\mathbf{r}, s) q(\mathbf{r}, N - s) \quad (4)$$

where N denotes the number of segments in the polymer. Moreover, the grand canonical partition function of the polymer solution can be expressed in the mean-field approximation as:[39]

$$\ln \Xi = \frac{1}{2B} \int d\mathbf{r}\; W^2 + Z \int d\mathbf{r} q(\mathbf{r}, s = N) \quad (5)$$

In the above equation, Z represents a nondimensionalized chemical potential for the polymer solution.

Overall, the above formalism provides a means to obtain the grand canonical partition function Ξ. In general, the above formalism also allows for incorporating a variety of physical polymer–particle interactions. Typically, such interactions manifest as appropriate boundary conditions on the diffusion eqn (3).[50,58,59] For instance, a purely impermeable wall is modeled as a boundary condition: $q(\mathbf{r}, s > 0) = 0$ on the surface. While effects of energetic interactions between the surface and the polymer can be incorporated directly as an external potential on the polymer segments, situations where the surface exhibits an extremely short ranged interaction (of range smaller than or comparable to the segment sizes), are usually modeled through a boundary of the form:

$$\mathbf{n} \cdot \nabla q(\mathbf{r}, s) = -\lambda q$$

on the surface. In the above, $\mathbf{n}$ denotes the normal to the surface, and λ^{-1} is a positive (negative) length scale quantifying the strength of attractive (repulsive) interactions.[44] An excellent discussion of the origin of boundary conditions and the associated numerical details can be found in the monograph by Fredrickson.[50] Solution of the SCFT equations with such boundary conditions allows one to determine $\Xi_n(\mathbf{r}_i, \mathbf{r}_j, \ldots, \mathbf{r}_n; z_p)$, which quantifies the grand canonical partition function of the polymer solution in the presence of fixed particles. In turn, this allows one to deduce the polymer-mediated interactions through eqn (1).

In general, the diffusion eqn (3) does not admit an analytical solution. Since our objective in this research was to specifically examine the phase behavior of polymer–nanoparticle mixtures for a range of particle sizes, especially for regimes where the curvature of the particle proves crucial in determining the physics, we solved the diffusion eqn (3) numerically.[39] This procedure was executed in spherical coordinates during the computation of $\Xi_1(Z, B)$ and in bispherical coordinates during the computation of $\Xi_2(\mathbf{r}_i, \mathbf{r}_j; Z, B)$. The use of a bispherical coordinate system allows us to access a wide range of particles sizes without encountering any artifacts arising from geometrical discretization errors. More details on the numerics of the method can be found in Roan and Kawakatsu.[60] In the next section, we

Published on 12 May 2010. Downloaded by University of Texas Libraries on 16/08/2013 15:20:49.

review the results of two classes of studies in which we have used the above formalism to model polymer–nanoparticle mixtures.

B. Nanoparticles in solutions with depleting polymers

Our first application of the above formalism was to study the interactions and phase behavior of nanoparticle–polymer mixtures for the case where the polymers and particles have no direct energetic interactions, except insofar as the polymers being only excluded from the interiors of the particles (commonly known as the "depletion" situation).[39] We note that this model is the simplest among the class of models characterizing the behavior of polymer-nanoparticle mixtures in which there are unfavorable enthalpic interactions between polymers and particles.[61] In such cases, it can be expected that polymer exclusion from the particle surfaces leads to an effective interparticle attraction between the particles which drives the aggregation and phase separation of particles. Prior theoretical research[62,63] had considered the magnitude of such depletion interactions in the "nanoparticle" regime, and had suggested that such depletion interactions were weak for small particles and that nanoparticle–polymer mixtures may be expected to be stable against demixing arising from such depletion attractions. Our research was specifically motivated to analyze these curvature effects in more detail due to experimental reports which contradicted with these theoretical considerations and demonstrated that in the nanoparticle regime smaller-sized particles may actually be more prone to phase separation than larger-sized particles.[64]

A model for depleting polymers was straightforwardly implemented in the context of the formalism described in section IIA by adopting a boundary condition $q(\mathbf{r}, s) = 0$ inside the surface of the particles.[50] This boundary condition embodies the impenetrability of the particle surface to polymer segments. Using such a formalism, in ref. 39 we analyzed the phase behavior of nanoparticle dispersions in polymer solutions. A first clue towards unraveling the peculiarities of the nanoparticle regime arose from considering the thickness of the polymer exclusion (depletion) zone around the particles (*cf.* Fig. 3a).[59,65] Explicitly, the latter showed that, in the nanoparticle regime, the volume of the polymer depletion layers can far exceed the size of the particles. Since the range of the depletion layers are also expected to determine the range of the *polymer-mediated* interparticle potentials, these results suggested that the nanoparticle regime may be accompanied by significant multibody interaction effects. Our hypothesis was that such multibody effects may render the effective interactions and phase diagram to be significantly different from what may be deduced by considerations of the infinite dilution situation involving a single particle.

To account for the above multibody effects, we proposed an approximate approach within the pair interaction formalism by rendering the chemical potential dependence Z of the polymer concentration C to also include a dependence on the particle volume fraction. The latter dependencies were in turn deduced using a free volume theory model for binary hard spheres.[66] The influence of such effects are displayed in Fig. 3b, which displays the particle volume fraction dependence of the pair-interaction potentials (for a fixed overall polymer concentration). It is clearly seen that while the polymer-mediated attractions are weak for dilute concentrations of particles, the polymer-mediated attractions become much stronger for nondilute concentration of particles. We translated such effects into a phase-diagram using a simple thermodynamic perturbation theory-like approach in which the polymer-mediated interaction potentials were treated as a perturbation to the bare interparticle hard sphere interactions. From the results displayed in Fig. 3c we observe that nanoparticle–polymer mixtures do indeed show a large region of immiscibility over a wide range of particle-polymer size ratios. It is also evident that for smaller particles, the decrease in particle size shifts the binodals monotonically toward lower concentrations of particles. The latter is indicative of more extensive immiscibility for smaller particles and provides strong evidence for the significance of the multibody effects incorporated in our model.

Overall, our above study highlighted several important aspects of depletion in nanoparticle-polymer mixtures which had not been addressed in earlier studies. Explicitly, considerations of the depletion characteristics (presented in ref. 39) suggested that the asymptotic results derived by the earlier theories are applicable only for either extremely small or extremely large particles and that crossover effects can play an important role in determining the interactions and phase behavior of intermediate-sized particles. More interestingly, our analysis suggested that while simple

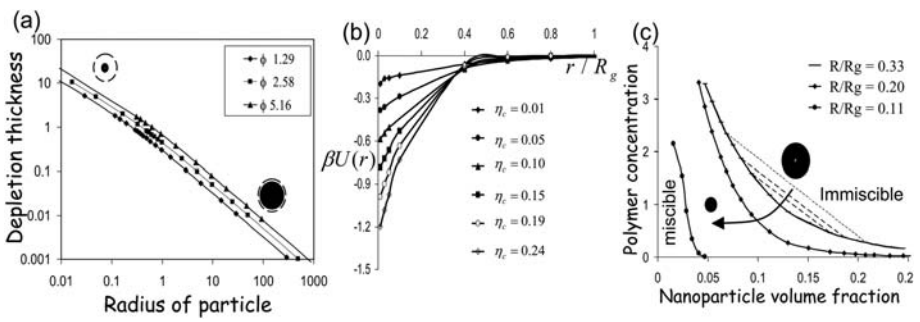

Fig. 3 (Results adapted with permission from ref. 39). (a) Depletion thickness of polymer layers (in units normalized by the radius of the particle R) as a function of the radius of the particle (in units normalized by the unperturbed radius of gyration of the polymer R_g). ϕ represents the polymer concentration normalized by the overlap concentration. (b) Particle volume fraction dependencies of polymer-mediated pair-interaction potentials $U(r)$ ($\beta \equiv 1/k_BT$) as a function of the distance between the particles r. The polymer concentration was maintained at $\phi = 0.2$ and the particle size $R/R_g = 5$; (c) Fluid–fluid coexistence curves for different particle sizes. The region above the lines represent the regions of immiscibility. The dashed lines represent the tie-lines for $R/R_g = 0.33$.

 This journal is © The Royal Society of Chemistry 2010

Published on 12 May 2010. Downloaded by University of Texas Libraries on 16/08/2013 15:20:49.

considerations based on surface tension effects (Fig. 2) may correlate to the miscibility at dilute concentrations, the overall phase behavior and dispersability in the nanoparticle regime may exhibit much richer characteristics. In the next section, we discuss another example where similar inferences are drawn.

C. Nanoparticles with adsorbing polymers

In a second application of our formalism,[44] we considered the phase behavior and mechanical properties of nanoparticle-polymer mixtures for which the particles have *favorable* enthalpic interactions with the polymer. This situation constitutes the common scenario where one may expect to achieve "dispersion" of the particles and is hence of significant interest for polymer nanocomposite applications. Yet again, our research was specifically motivated by the interplay between polymer–particle interactions and the particle curvature in determining the phase behavior and the particle structure in such situations.

The potential richness of the phase behavior and the impending curvature effects becomes manifest when considering both the polymer concentration and particle size dependence of polymer-mediated interparticle interactions (at infinite dilution, obtained using the formalism described in section IIA) displayed in Fig. 4a and b. For the case of a particle size ratio $R/R_g = 0.5$, we observe that for dilute bulk polymer concentrations ϕ_{bulk}, the interaction potentials are monotonically attractive as a function of interparticle distance. At such dilute polymer concentrations, effects arising from interpolymer interactions are expected to be relatively weak. Consequently, when two particles are brought closer, the polymers are free to adsorb, form more interparticle bridges and gain energy without incurring concomitant entropic costs. These effects lead to a strong, monotonic attraction between particles at low ϕ_{bulk}. Upon increasing the ambient polymer concentration, the interactions develop a nonmonotonic character, displaying attraction at large interparticle separations followed by a repulsive behavior at smaller interparticle distances. At even higher bulk concentrations, it is seen that the interactions become monotonically repulsive with the interparticle distance. The above changes in the character of the interparticle potentials may be rationalized as arising from an

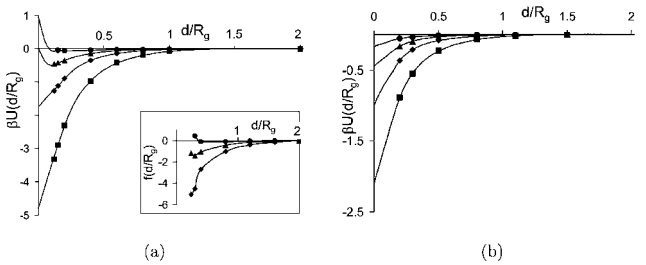

Fig. 4 (Figures adapted with permission from ref. 44). (a) Pair interaction potentials as a function of interparticle distance d (normalized by polymer radius of gyration R_g) for polymer-to-particle size ratio $R/R_g = 0.5$. Bulk concentrations are $\phi_{bulk} = 1.29$ (■), 2.58 (◆), 3.87 (▲), 5.16 (●) where ϕ_{bulk} represents the bulk polymer concentration normalized by the overlap concentration. The inset shows corresponding interparticle forces as a function of interparticle distance d/R_g for $\phi_{bulk} = 1.29$, 2.58 and 3.87. (b) Corresponding pair interaction potentials for $R/R_g = 0.25$.

increase in the interpolymer interactions arising from the osmotic confinement effects and more importantly the saturation of the surfaces by the adsorbed polymers. Together these effects lead to the repulsive interactions noted for intermediate and concentrated situations.

If we consider the influence of the size of the particle upon the characteristics of the pair interaction potentials (*cf.* Fig. 4b), we observe that the interaction potentials become weaker with decreasing size of the particles. To rationalize this, we recall from our above discussion that the magnitude of the attractive interactions are determined by the number of bridging segments between the particles. A smaller particle has smaller surface area leading to the formation of lesser number of bridges. The decrease in bridging can be argued to be the underlying cause of the overall weaker attraction between the particles.

It is interesting to note that the above results contradict the conclusions one may derive based on the surface tension results displayed in Fig. 2. Indeed, situations of favorable polymer–surface interactions were expected to lead to negative surface tension and promote dispersability. In contrast, the above results suggest that such situations are accompanied by strong polymer-mediated interparticle attractions and potential immiscibility. To delineate the physics of such polymer-nanoparticle mixtures, in ref. 43 we translated the above interaction potentials to phase diagram predictions by using a thermodynamic theory very similar to the one employed in the context of depletion interactions (section IIB). Figs 5a and b display the corresponding results which include regions of immiscibility as delineated by the fluid-fluid coexistence curves for particle sizes $R/R_g = 1.0$ and 0.25. For all the particle sizes, we observe generically a fluid phase at low polymer concentrations (below the schematic lower boundaries indicated by dashed lines), followed by bridging-induced phase-separation at higher polymer concentrations and subsequently a stable mixture regime at even higher polymer concentrations. The latter stabilization arises as a consequence of the saturation of the adsorption and the repulsive interactions at the higher polymer concentrations.

It is evident by comparing Fig. 5a and b that the relative polymer-particle sizes play an important role in influencing the structure and phase behaviors. At dilute particle concentrations, we observe that a lowering of the R/R_g ratio shifts the upper boundary of the two phase region to lower polymer concentrations. The latter suggests that polymer-nanoparticle mixtures involving smaller particles at dilute particle concentrations tend to become miscible at much lower polymer concentrations compared to the larger particles. A second particle size effect is observed in the compositions of the coexisting phases denoted through the tie lines (shown by the lighter lines). We observe that for larger particles, the concentrations of polymer in the two coexisting phases are more or less the same. The latter suggests that the phase separation in such systems forms a particle-rich and particle-depleted phase, both rich in polymers. On the other hand, for smaller particles, the phase separation is into a supernatant phase that is dilute in both the polymer and the particles, whereas the "floc" phase is rich in both the polymer and particles. The latter trends are consistent with the phenomena of "complex coacervation" commonly observed in the context of protein–polysaccharide mixtures.[67–69]

Published on 12 May 2010. Downloaded by University of Texas Libraries on 16/08/2013 15:20:49.

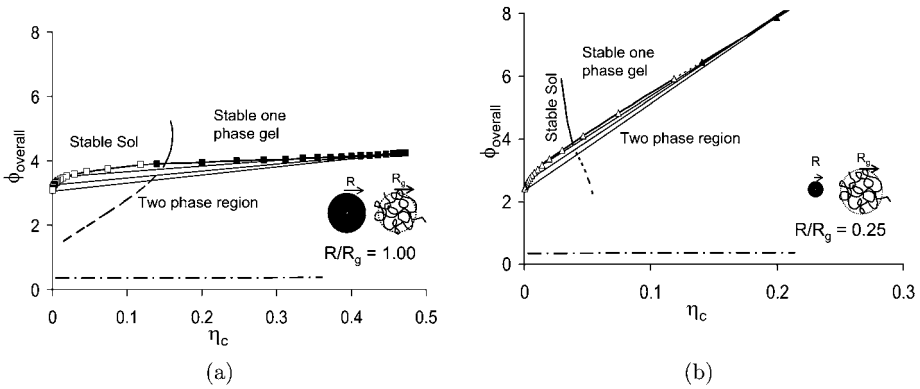

Fig. 5 (Figures adapted with permission from ref. 44). Fluid–fluid co-existence curve (open and filled symbols) and percolation line (solid line continued as a dotted line into the region of coexistence) in the polymer concentration ($\phi_{overall}$)–particle volume fraction (η_c) plane. The area above the co-existence curve shows the one phase region and that below each curve represents the two phase region. The compositions of the coexisting phases are shown by tie lines joining the "floc" (filled symbols) and supernatant (open symbols) compositions. The lower boundary for the two phase region is displayed schematically by dash-dot line. Area to the left of percolation line shows fluid phase and that to the right represents percolated phase: (a) $R/R_g = 1.0$; (b) $R/R_g = 0.25$.

In many applications involving nanoparticles, such as in their use as rheological modifiers, more detailed information regarding the polymer–particle floc complexes and their mechanical properties is also desired.[67–69] To address these issues, we developed a new simulation strategy[41,43,69,70] in which the above framework was first extended to deduce the probability of forming polymer bridges between two particles. Subsequently, a semi-grand canonical Monte Carlo simulation was implemented using the polymer-mediated effective interparticle potentials while mapping out the connectivity of the particles using such bridging probabilities. Knowledge of the connectivity allowed us to quantify the cluster sizes of polymer-bridged particles and the resulting mechanical strength of such complexes through simple elastic network theories. In Fig. 6 we display the results obtained using this idea which provided for the first time quantification of the percolation, complexation thresholds and mechanical strengths in such mixtures.

In summary, the above-discussed situation again provides an interesting illustration of the idea that single particle miscibility considerations, while useful, may not necessarily provide a complete picture of the dispersability and the resulting structure of the polymer-nanoparticle mixture.

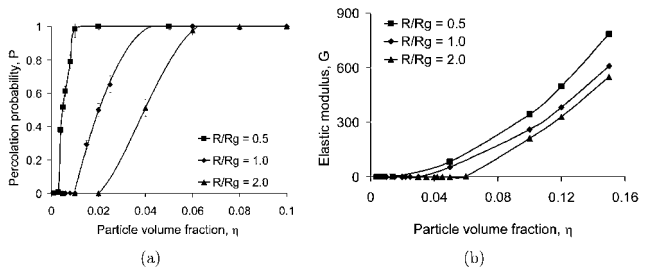

Fig. 6 (Figures adapted with permission from ref. 41): (a) Percolation probabilities (P) for the polymer-bridged particle gels displayed as a function of particle volume fraction, η, for different particle-to-polymer size ratios, R/R_g = 2.0, 1.0, 0.5 for a polymer melt matrix; (b) elastic modulus (G') (deduced using a network theory for elasticity) as a function of particle volume fraction, η, for particle-to-polymer size ratios, R/R_g = 2.0, 1.0, 0.5 for a polymer melt matrix.

D. Applications to anisotropic fillers

In more recent studies we have extended our formalism to study the effective pair-interaction potentials and the resulting phase behavior and percolation transitions of *nanorods* dispersed in solutions of adsorbing polymers.[47] We again used a polymer self-consistent field theory (SCFT) framework in conjunction with a Derjaguin approximation to compute the polymer-mediated orientation-dependent pair interaction potentials between cylindrical nanorods. A modified Flory theory and a simple analytical model were then used to deduce the different equilibrium phases and the onset of percolation for nanorods in polymer solutions.[71,72] Yet again, rich phase behavioral characteristics, including the possibility of isotropic and nematic phases, were deduced. We delineated results quantifying the influence of polymer-surface affinity, polymer concentrations, radius of rods, and aspect ratio of rods, on the topology of such equilibrium phases and percolation regimes.

E. Other related theoretical studies

Considering the significant practical ramifications, theoretical models and computer simulations for predicting the phase behavior of polymer–nanoparticle mixtures has attracted significant interest. Of this research, the issue of "depletion" interactions in polymer solutions has specifically involved many modeling and simulation studies in both the physics and the materials sciences communities. The origin and nature of depletion interactions were first elucidated over 50 years ago by Asakura and Oosawa (AO),[73] and independently by Vrij.[74] The AO model is known to be adequate only for the case of *dilute and noninteracting* polymer solutions and only when the radius of gyration R_g is much smaller than the size R of the particle. Subsequently, many studies have examined the depletion characteristics in particle–polymer mixtures for situations beyond these limiting constraints. For instance, Meijer and Frenkel[75]

 This journal is © The Royal Society of Chemistry 2010

Published on 12 May 2010. Downloaded by University of Texas Libraries on 16/08/2013 15:20:49.

used a lattice simulation approach to analyze the case of dilute, ideal polymer solutions with larger polymer to particle size ratios, and showed that multibody interactions between the particles can lead to significant corrections to the phase behavior predicted by the AO theory. Schweizer and coworkers[76–81] pointed out the breakdown of AO theory for the regime $R_g/R \approx O(1)$, and have subsequently developed integral equation approaches which incorporate the interactions between the polymers and treat a wide range of polymer and particle sizes. Bolhuis, Louis and coworkers have developed a novel coarse-graining technique to treat the case of interacting polymers for sizes R/R_g upto $O(1)$.[82,83] Both Schweizer's and Bolhuis *et al.*'s researches established the importance of interpolymer interactions, and also delineated the resulting phase behavior for a variety of parametric conditions. Lekkerkerker, Tuinier and coworkers[66,84–87] have pioneered the Gibbs adsorption and free volume theories to develop the phase diagrams for mixtures of colloids of different geometrical shapes in both ideal and interacting polymer solutions. Also, alternative approaches invoking perturbation theories,[88] and cell models[89] have been used to predict the phase behavior of nanoparticle–polymer solutions characterized by depletion interactions.

In contrast to the above depletion situation, there have been far fewer theoretical studies quantifying the influence of favorable enthalpic interactions between the polymer and the particle surface. The earliest studies in this regard were based on scaling theories designed to address the adsorption and interaction characteristics of polymer solutions on flat plates and large colloidal particles.[59,58,90,91] Various molecular modeling techniques such as density functional theories[92] and integral equation theories[93] were also successfully applied to extract the detailed structural descriptions and thermodynamic properties of polymer solutions in the presence of flat surfaces. Extensions to the nanoparticle regime have mainly been at a scaling level and relate only to the adsorption characteristics on a single nanoparticle.[94,95]

More pertinent to the PNC applications are studies considering the interaction and phase behavioral characteristics of nanoparticles in polymer melts.[36] The earliest studies specific to the polymer melt context came from the groups of Gianellis[96] and Balazs and coworkers,[97] who used polymer self-consistent field theory to analyze the thermodynamics of mixing between polymer and clay-like fillers. Their results pointed to the interplay between entropic polymer conformational effects and polymer-filler energetic interactions in controlling the equilibrium state of polymer-clay mixtures. Subsequently, in a series of articles,[98,99] Balazs and coworkers extended the above studies by combining polymer self-consistent field theory with density functional theories to predict complete phase diagrams for mixtures of polymers and plate and rodlike particles in a polymer melt, which among other predictions also delineated optimal conditions for creating stable dispersed composites.

Use of integral equation theories for addressing the above issues in the context of polymer melts has been pioneered by Schweizer and coworkers.[36,53,100,101] Such theories can accommodate a finer representation of the polymer chains relative to coarse-grained elastic thread models and can hence yield information regarding polymer packing and particle structure while incorporating the multibody particle effects (albeit, in an approximate manner). Specifically Schweizer and coworkers have adapted the PRISM theory[101,53] to investigate the equilibrium miscibility, particle dispersion and phase separation of polymer-particle mixtures and polymer nanocomposites. They have used this formalism to examine the influence of particle size, degree of polymerization and melt density upon the structure, effective forces and thermodynamics of polymer nanocomposites. A notable prediction from such theories is the possibility of two distinct kinds of phase separation behaviors in mixtures of particles and polymer melts. The first occurs at lower monomer-filler attraction strength which corresponds to an entropic depletion attraction-induced phase separation. The second regime occurs at a higher monomer-filler adsorption energy and involves the formation of an equilibrium physical network phase with local bridging of fillers by polymers. Selected applications of the PRISM framework to PNCs have been summarized in a recent review article.[36]

Direct computer simulation approaches have also been used to address the equilibrium structure and phase behavior of mixtures of spherical nanofiller units dispersed in homopolymers.[33,102–110] Specifically, Smith and coworkers[33] and Keblinski and coworkers[106] used molecular dynamics simulations to study the effective interactions between two spherical nanoparticles in a polymer melt. These studies quantified the magnitude of effective interactions as a function of different physical parameters including the interaction strength between the polymer monomers and the particle. De Pablo and coworkers[111,112] have used molecular simulations to analyze the depletion interaction and deduce the effective polymer-mediated interactions between colloidal particles. Their results were consistent with earlier theoretical predictions except insofar as monomer level and chain length effects not captured in coarse-grained mean-field theories.

III. Mixtures of homopolymers with grafted nanoparticles

In this section, we briefly review some of the developments in the context of coarse-grained modeling of *functionalized nanoparticles* dispersed in homopolymer melts. As noted in the introduction, functionalization of particles is a common, and in many cases the only viable strategy to facilitate the dispersion of nanoparticles in polymer matrices. Experimentalists have explored the use of two broad classes of functionalizers in these efforts: (i) anionic or cationic oligomeric surfactants;[26,30,113] and (ii) grafted polymers.[114–117] In modeling the effect of small molecule surfactants, we note that at the level of coarse-grained modeling, such surfactants are typically at the same scale as that of a single coarse-grained polymer unit. Consequently, as a first approximation, the conformational degrees of freedom of the surfactant may be ignored, and phase behavior of nanoparticles functionalized by such surfactants may be mapped onto the behavior of polymer–particle mixtures in which the surfactant effects manifest just as effective enthalpic interactions between the polymer and particle (the results for the latter situation was discussed in section II C). On the other hand, for modeling situations where the nanoparticles are grafted with either a polymer or longer surfactants, the conformational degrees of freedom of the grafted functionalizer need to be accounted for in

Published on 12 May 2010. Downloaded by University of Texas Libraries on 16/08/2013 15:20:49.

quantifying the interactions and phase behavior of the resulting mixture. In the following, we briefly review the developments that have accompanied the latter context. Without loss of generality, we refer to the functionalizers as polymers with the understanding that they may equally well be a longer molecule surfactant.

The simplest model system which has attracted the most attention from both an experimental and theoretical perspective is one where the grafted polymer is chemically identical to the matrix polymer (termed the "autophobic" case). In such cases there are no *competing* enthalpic interactions, and the polymer-mediated interactions and phase behavioral characteristics arise primarily from the entropic effects pertaining to the grafted polymer and the matrix chains. Much of the theoretical developments in this area have grown out of the seminal descriptions of the wetting and dewetting of polymer melts on polymer brushes advanced by Leibler and coworkers.[118,119] Explicitly, using scaling ideas and strong segregation theory calculations they delineated the regions where the matrix polymer wets or dewets the brush. In the former case, the matrix chains completely penetrate the brush, whereas in the latter case the matrix chains are either expelled or penetrate only a finite zone into the grafting layer (*cf.* Fig. 7).[119] From the diagram of states displayed in Fig. 7c, it can be seen that the overall behavior depends on the degree of polymerization of the grafted chains, N, the chain grafting density σ, and the degree of polymerization of the free host chains, P. Explicitly, when $\sigma\sqrt{N} > (N/P)^2$ dewetting of the melt chains is expected ("dry" brush). In other words, situations involving long matrix polymers and/or densely grafted polymer functionalizers would be more conducive to dewetting. We also note that while these considerations were derived based on scaling arguments and analytical theories, Matsen and Gardiner have carried out careful SCFT based numerical analysis of these issues.[120] Their results have confirmed many of the above details at a qualitative level with however some significant quantitative differences which highlight the approximations inherent in analytical theories.

To translate the above considerations to the dispersion of nanoparticles,[121] we observe that the case of "dewetting" is akin to the polymer "depletion" case, and hence one may expect that for extreme cases of dewetting the matrix polymer-mediated interparticle interactions become attractive, and lead to aggregation and phase separation of the particles. In contrast, the "wetting" situation is similar to one where the matrix polymers possess favorable enthalpic interactions with the particles (except insofar as the absence of polymer bridges), and hence the interparticle interactions and phase behavior may be expected to favor dispersion or mixing. Such considerations were first confirmed in a combined theoretical and experimental work by Hasegawa and coworkers who calculated the interplay between the brush–brush repulsions and the emergence of dewetting-induced attractive interactions.[114] An interesting optimum intermediate grafting density was predicted where the net attractions were weakest and the particles are most well-dispersed. More recently, systematic experiments by Green and coworkers and others have confirmed the correspondence

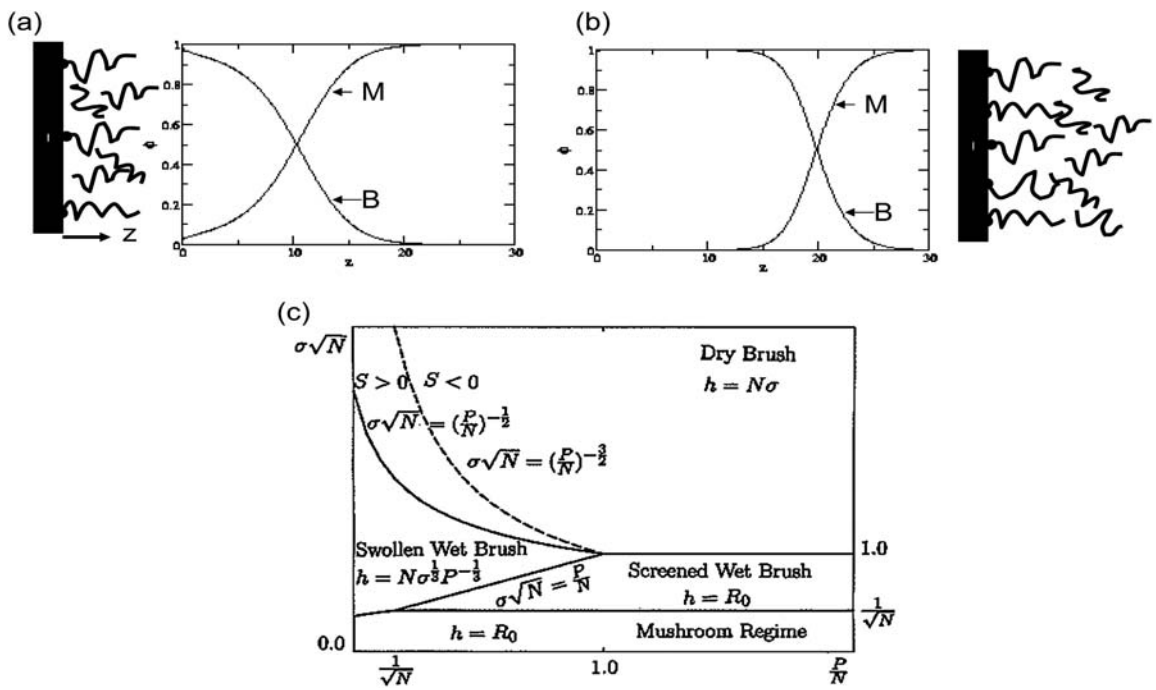

Fig. 7 (a) and (b) A schematic of the wetting to dewetting transition in the interfaces between melt and polymer brushes. The wetting regime corresponds to the penetration of the melt chains into the brush. In contrast, the dewetting regime corresponds to either the partial penetration or complete expulsion of the melt chains from the brush. These behaviors are indicated schematically also in the volume fraction profiles of the melt (M) and brush chains (B). (c) (Reproduced with permission from ref. 119) Diagram of wetting-dewetting transitions in (N, P, σ) plane for a polymer brush of polymerization index N immersed in a melt of the same polymer with a different polymerization index P. The full lines are the boundaries between the regions with different scaling laws for the brush height, h. The dashed line separates the two regimes of scaling of the brush-melt interfacial thickness and coincides with the frontier between the regions of positive and negative spreading coefficients.

 This journal is © The Royal Society of Chemistry 2010

View Article Online

Published on 12 May 2010. Downloaded by University of Texas Libraries on 16/08/2013 15:20:49.

between the wetting–dewetting transitions and the miscibility behavior of grafted nanoparticles.[122–124]

While much of the above-discussed studies were based on results obtained by considering the behavior of flat grafted surfaces (in conjunction with possibly Derjaguin approximations), very recently density functional theories,[125,126] SCFT approaches[127,128] and computer simulations[129–132] have started tackling the particle curvature effects in a much more direct manner. For instance, the interaction between two brush coated spheres in a good solvent has been studied to confirm its purely repulsive nature.[128,125] Other density functional studies and simulations[125,133] have also examined the influence of solvent quality effects, and have suggested that richer interaction characteristics including attractions and repulsions are possible depending on the solvent quality. Recent SCFT studies for grafted nanoparticles in polymer melts have also examined in more detail the effects of particle size and grafting density upon the interparticle interactions (albeit, for a specific ratio of grafted and free polymers chain lengths).[134] The latter studies point to the applicability of considerations gleaned from the studies on flat plates, with however much weaker interactions and a particle size, grafting density dependent shift of the wetting–dewetting regimes for curved surfaces. The implications of such weaker interactions for the context of dispersion of nanoparticles have been examined using a simple theory by Harton and Kumar.[135]

Another independent line of investigation has been initiated by Schweizer and coworkers focusing on the use of integral equation theories to shed light on the behavior of "sparsely grafted" nanoparticles (with only a few grafted chains) dissolved in a homopolymer matrix.[36,136–139] PRISM theories have gone beyond many above-mentioned studies by considering the effects arising from finite concentration of particles. Interestingly, they predict that melts and dense solutions of nanoparticles may exhibit signatures of "microphase ordering" (in addition to the possibility of macrophase demixing) accompanied by the formation of structural characteristics at a finite length scale.

A. Some future directions

In concluding this section, we mention two issues which have received far less attention in the context of dispersing polymer functionalized nanoparticles in polymer melts:

(i) A complete theoretical understanding of the interactions and phase behavior of polymer grafted nanoparticles dispersed in homopolymer melts requires consideration of a vast parameter space in which the molecular weight of the grafted polymer and its chemical identity need to be accounted in addition to effects arising from the particle size, the particle's interactions with the polymer matrix and the molecular weight and/or concentration of the matrix polymer. The studies discussed in the preceding section have clarified the roles of the relative sizes of the matrix and grafted polymer lengths, grafting densities and (to a more limited extent) the curvature of the particles. However, an issue which has attracted less attention has been the role of chemical mismatch between the matrix and grafted polymers. Indeed, the parameter space available to synthetic chemists is considerably enhanced if polymers chemically distinct from the matrix polymer are used to functionalize and disperse the particles.

A seminal study in the above regard was carried out by Borukhov and Leibler, where the tethered and matrix polymers were allowed to be chemically distinct but with favorable interactions (the brush-matrix Flory interaction parameter was chosen to be negative).[140,141] They used scaling arguments to show that under appropriate conditions this may serve to eliminate the effective attraction (and potential immiscibility) noted in the case where the matrix polymers are chemically identical to the grafted chains. More recently, we have examined the wetting characteristics of polymers which are chemically different and possess unfavorable interactions with the brush component.[142] We reported experimental results and complementary strong-segregation theory arguments on the parametric interplay between enthalpic and entropic effects in the interfaces between polymers and polymer brushes. Our studies indicated (*cf.* Fig. 8) that one may be able to use brushes made of incompatible polymers of sufficiently high molecular weight and achieve lower interfacial tensions compared to brushes made of compatible polymers of small molecular weight. Since overall particle dispersability usually correlates to the melt-brush interfacial tensions, this strategy may open the door to more functionalization possibilities when synthesis and/or grafting methods prove to be limiting.

(ii) A second issue relates more closely to the theme of the studies discussed in the previous sections, *viz.*, behavior arising at nondilute concentrations of nanoparticles. Indeed, most of the studies mentioned above (except the recent PRISM efforts) relate to either the wetting/dewetting considerations or the interactions arising in the context of two particles. While such results provide valuable guidelines for dispersion strategies, the structure resulting in the multiparticle situation may potentially exhibit much richer features. A recent example of this effect was noted in the context of experiments and related theoretical studies on dispersing spherical nanoparticles grafted with polymeric brushes into a homopolymer matrix (see Fig. 9).[143,144] The

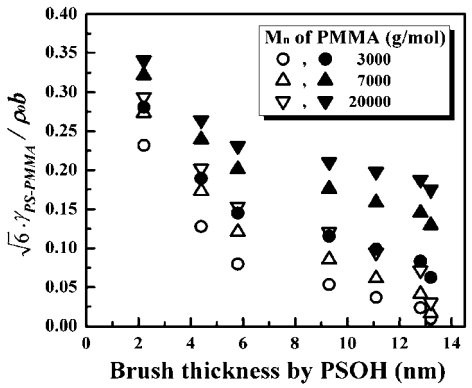

Fig. 8 (Reproduced with permission from ref. 142) Strong segregation theory calculations of interfacial tension $\gamma_{PS-PMMA}$ between polystyrene brush and a poly(methyl methacrylate) (PMMA) melt for different M_n of the PMMA polymer melt. ρ_0 and b respectively denote the monomeric volume and the segment length of the polymer. The closed symbols were computed using a Flory–Huggins interaction parameter $\chi \equiv \chi_{PS-PMMA} = 0.037$. The open symbols used $\chi = 0$ which corresponds to the "autophobic" case. It is evident that in practice one may be able to use brushes made of incompatible polymers of sufficiently high molecular weight and achieve lower interfacial tensions compared to brushes made of compatible polymers of small molecular weight.

Published on 12 May 2010. Downloaded by University of Texas Libraries on 16/08/2013 15:20:49.

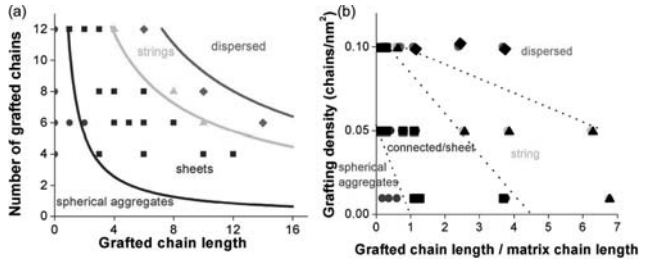

Fig. 9 (Adapted with permission from ref. 143) Parametric phase diagram for the structures formed during the dispersion of polymer grafted nanoparticles in a polymer matrix. The matrix polymer was kept the same while the number and size of the grafted polymers were varied. (a) A comparison of theoretic calculations based on strong-segregation theory (solid lines) and simulations (points). Spherical symbols: spheres, square symbols: sheets, triangles: strings, diamonds: well-dispersed particles; (b) Experimental 'morphology diagram' of polymer-tethered particles mixed with matrix polymers. Spherical symbols: spheres, square symbols: sheets, triangles: strings, diamonds: well-dispersed particles. The lines that separate the different regions are merely guides to the eye (see ref. 143 for details on the experimental system).

theoretical ideas were based on simple scaling models to enumerate the free energies of the different structures observed in computer simulations (and experiments). Explicitly, it was proposed that the equilibrium structures were chosen as a result of the competition between the entropic penalty arising due to the conformational rearrangements of the grafted chains and the enthalpic gain arising from the bare particle–particle attractions. Even within the "wetting" regime, we noted that the preceding interplay between can lead to novel self-assembly of the particles into anisotropic structures. While this study was just an isolated example highlighting the issues, the rich characteristics of the multiparticle assembly and phase behavior for the full parameter space of dispersion of polymer-grafted particles in polymer melts still remains to be elucidated.

IV. Self-assembly of nanoparticles in block copolymer matrices

Recently, the lessons learned from efforts to maximize dispersion of nanoparticles in homopolymer melts have been furthered towards "dispersion control" which focuses on directing the self-assembly in nanoparticle-block copolymer mixtures. These ideas have led to a surge of experimental reports which exploit the self-assembly in mixtures of diblock copolymers and nanosized particles to produce ordered organic-inorganic hybrid materials.[7,145–151] In some applications, the microphase separation of the block copolymers is used as a template to control the ordering of the particles and to produce highly organized hybrid materials.[145–147,152] The possibility of using such strategies to achieve significant loading of nanoparticles has also been demonstrated.[153] In other applications, the particles are used to modify the self-assembly of the parent block copolymer to lead to new morphologies of self-assembly.[154,155] The resulting structures have been proposed for use in applications such as separation processes, next-generation catalysts and photonic band gap materials.[7,152]

For successful fruition of the above applications, a fundamental understanding of the manner in which different parameters in such systems, such as the size, shape, volume fraction of particles, copolymer composition, and interaction energies between the different components control the thermodynamics and self-assembly of such nanoparticle-block copolymer mixtures. Nanoparticle-block copolymer composites represent another facet in the category of nanoparticle-polymer mixtures where simple concepts such as the surface tension effects (*cf.* Fig. 2 and the accompanying discussion) alone are not expected to provide a complete understanding of the richness of the phase behavior and dispersion characteristics. Indeed, the overall self-assembly in such systems is expected to depend on an intricate interplay of such surface tension effects with the energetic effects driving the block copolymers to self-assemble. In this section, we briefly review some of the theoretical developments which have occurred used coarse-grained modeling and simulation to clarify these effects in the context of nanoparticle organization and self-assembly in block copolymers.

A. Templated organization of nanoparticles in self-assembled phases of block copolymers

In many applications, it is desired to achieve templated organization, in which the nanoparticles are either directed to the interface or to exist wholly within one of the phases of the self-assembled block copolymer phases. A fundamental question confronting such strategies is: "what are the physical parameters controlling the nanoparticle distributions in block copolymers?" This question was first addressed using modifications of SCFT theories by Balazs,[37] and then subsequently by using molecular dynamics,[156] Monte Carlo framework[157] and a hybrid field theory based simulation approach.[38] Broadly, the results of these studies suggested that the templating of the particles by the block-copolymer is dependent on the size of the particles and their interactions with the different units of the copolymer. If the particles were compatibilized to just one of the components ("selective" particles), then they were predicted to localize at the center of their preferred phase, while particles compatible to both components ("nonselective" or "surfactant-like" particles) were predicted to localize at the AB interface of a AB diblock copolymer.

In recent work, we used strong-segregation approximation to develop an analytical theory which provides a mechanistic basis and identifies the important parameters governing the above results of particle distributions.[42] Explicitly, we argued that there were three primary energetic factors whose interplay governed the particle distributions: (i) particles positioned at the interface of the copolymeric phases decrease the interfacial contacts between the blocks and lower the accompanying interfacial energy costs; (ii) particles positioned in their preferred phase (*i.e.* the phase to which the particles possess relatively more favorable enthalpic interactions), gains in energy; and (iii) location of the particle within the brush-like block copolymer phases incurs elastic energy costs arising from the distortion of the brush chains. These elastic costs are expected to be largest in magnitude near the interface of the blocks (the "grafting" location) and weakest at the locations which are furthest from the interfaces.

 This journal is © The Royal Society of Chemistry 2010

Published on 12 May 2010. Downloaded by University of Texas Libraries on 16/08/2013 15:20:49.

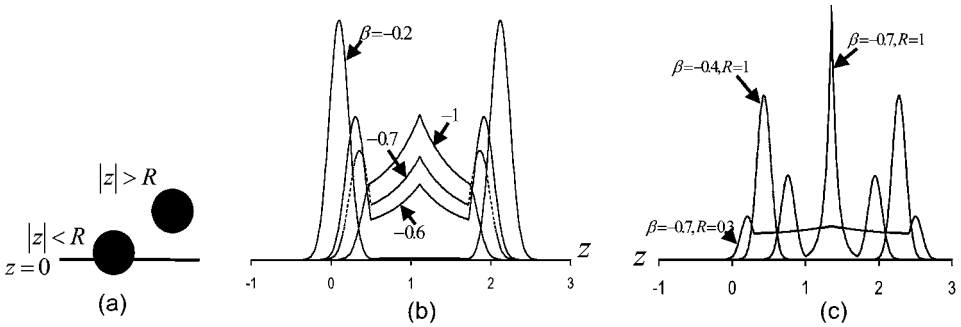

Fig. 10 (a) A schematic of the particle configuration relative to the AB interface (denoted by the plane $z = 0$). (Adapted with permission from ref. 42): (b) and (c) Probability distribution of the nanoparticle location in the block copolymer lamella as a function of the selectivity parameter β and the particle size R in R_g units. In (b) the particle size $R = 0.5$. z denotes the distance normal to the plane of the AB interface (in R_g units) with $z = 0$ corresponding to the AB interface. $z \simeq 1$ corresponds to the center of the A layer).

To render the above arguments concrete, in the following, we consider the lamellar phase of a symmetric AB diblock copolymer and denote the particle radius as R. We take a coarse-grained view where the interactions between the particle and the A and B components of the polymer are quantified respectively by two interfacial tension parameters denoted η_{AC} and η_{BC}. The parameter $\delta\eta = (\eta_{AC} - \eta_{BC})$ represents the "selectivity" of the particle to the polymer component (for $\delta\eta < 0$, the particles are preferential to the A phase). By denoting η_{AB} to be the interfacial tension between the A and B phases, the energetic terms (i) and (ii) above can be estimated as a function of the nanoparticle location z (*cf.* Fig. 10a) relative to the AB interfacial plane as

$$F_{\text{enth}}(z) = \begin{cases} \pi(z^2\eta_{AB} + 2Rz\delta\eta)\,, & |z| \le R \\ \pi R^2\left(\dfrac{2z\delta\eta}{|z|} + \eta_{AB}\right), & |z| > R \end{cases} \tag{6}$$

In the above, the two distinct cases arise from the reduction in the AB interface when the particle is positioned such that $|z| < R$, and the lack of such an effect for $|z| > R$. The term (iii) above can be estimated using the results of Williams and Pincus[158] and the more recent work of O'Shaughnessy and Kim[159] as

$$\Delta E_{\text{br}}(z) \simeq P(z)\frac{4\pi R^3}{3} \tag{7}$$

where $P(z)$ denotes the osmotic pressure field acting on the segments of a polymer brush at a location z. Using eqn (6) and (7), we can approximate the density distribution of nanoparticles $\rho_C(z)$ in the diblock lamella as:

$$\rho_C(z) \propto \exp\left[-F_{\text{enth}}(z) - \Delta E_{\text{br}}(z)\right]. \tag{8}$$

By using expressions from strong segregation theory for $P(z)$ and η_{AB} we can deduce the parametric dependencies of the density distribution of the nanoparticles.[42,159] In the following, we briefly discuss (*cf.* Fig. 10b and c) the results obtained as a function of the parameter $\beta = \delta\eta/\eta_{AB}$ (β^{-1} quantifies the degree of amphiphilicity or the surfactant-like nature of the particle) and the size R. From Fig. 10b, it can be seen that for a fixed R, small values of β lead to a localization of the particles at the AB interface of the copolymer. In contrast, increasing the selectivity

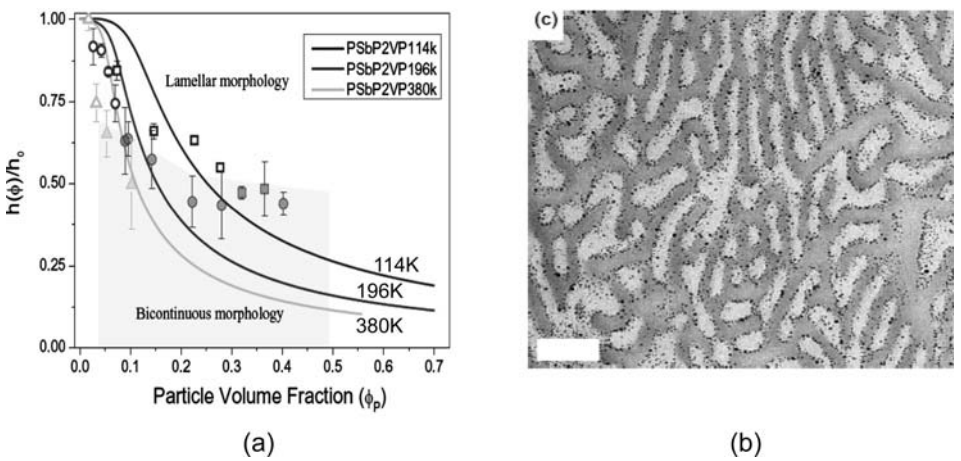

Fig. 11 (Adapted with permission from ref. 154) (a) The volume fraction (ϕ) dependence of lamellar thickness $h(\phi)$ (normalized by the values at zero particle concentration h_0) for PS-*b*-P2VP diblock copolymers with M_n values of 114 kg mol^{-1} (squares), 196 kg mol^{-1} (circles), and 380 kg mol^{-1} (triangles). The lines (M_n values indicated) correspond to the predictions of strong segregation theory. (b) Cross-sectional TEM images of PS-*b*-P2VP block copolymer (M_n 196 kg mol^{-1}) containing PS–Au nanoparticles at a volume fractions of 0.09. It is evident that the microstructure of the PS and P2VP domains becomes bicontinuous.

Published on 12 May 2010. Downloaded by University of Texas Libraries on 16/08/2013 15:20:49.

of the particles leads to a delocalization of the particles into their preferred phase. Interestingly, we observe that for intermediate values of selectivity, the overall density distribution displays three peaks corresponding to a localization at the middle of the brush in its preferred phase. The latter is a manifestation of the interplay between the lower elastic energetic cost associated with the particle being present at the top extremities of a polymer brush compared to its interiors and the interfacial energy gain in localizing at the interface.

Size effects are presented in Fig. 10(c). It can be seen that small selective particles are predicted to be more localized at the AB interface, whereas the larger particles tend to exhibit more preferential segregation. These effects can be rationalized as arising from the fact that the interfacial tension gain (eqn (6)) scales as R^2 (surface area) whereas the elastic energy cost (eqn (7)) scale as R^3 (the volume of the particle). Consequently, for small particles and/or for stronger segregation between A and B phases (*i.e.* larger AB interfacial tension), the particles can be expected to be more localized at the AB interface. In contrast, for larger particles and/or weaker segregations, the tendency to segregate into the preferred domain dominates.

A related outcome of the above analysis was the prediction that the addition of "surfactant-like" nanoparticles (*i.e.* with selectivity $\delta\eta \simeq 0$) are expected to contract the lamellae and lower the elastic constants of the block copolymer. Both these effects can be physically understood as arising from the reduction in the AB interfacial costs arising from the positioning of the particles at the interface. Hence, the chains have to stretch less to accommodate the unfavorable AB contacts. A quantitative analysis of such effects also suggested that lowering of the elastic modulii may lead to the nanoparticle-induced creation of bicontinuous phases in the block copolymer. Shown in Fig. 11 are experimental results confirming such predictions.[154]

In closing, we note that the above considerations were based on analytical arguments founded on strong-segregation theory calculations. More recently, Kim and Matsen have presented a careful quantitative analysis of the particle distributions using a novel numerical implementation of the SCFT formalism.[160–162] While their results for the bare particles are qualitatively consistent with the arguments presented in ref. 42, they have also extended these considerations further by treating accurately the influence of polymeric functionalizers.

B. Self-assembly in block copolymer nanoparticle composites

The developments discussed in the preceding section pertain to the physics of templated assembly of nanoparticles in block copolymer matrices. However, a full understanding of the morphology of the block copolymer-nanoparticle composites must accommodate the possibility of both particle self-assembly as well as particle-induced modifications of the block copolymer self-assembly. Seminal steps towards a theoretical description of this problem was taken by Balazs and coworkers, who extended the self-consistent field theory of multicomponent polymers to include the presence of hard particles of different shapes and delineated the resulting particle and block copolymer self-assemblies for a variety of physical parameters which included confinement effects.[37,163–167] Broadly, the results of their analyses suggested a rich self-assembly behavior determined by an interplay between the shape, size and selectivity of the particles and the other physicochemical features of the block copolymers. Recently, molecular dynamics simulations,[156] cell dynamics based approaches,[168] density functional theories[169] and Monte Carlo simulations[170,171] have also been used to study similar issues. These studies have suggested phase behavior that is qualitatively consistent with the predictions of the SCFT theory of Balazs and coworkers.

C. Some future directions

While a number of advances have been reported recently in the theoretical modeling and simulations of the interplay between nanoparticles distributions and the self-assembly in block copolymer phases, a question which is yet only partially resolved is the impact of surfactants and polymeric functionalizers in the assembly of nanoparticles in block copolymer phases. In situations where the functionalizers are small molecule surfactants, their influence may be subsumed within effective energetic parameters, and models reviewed in the preceding sections may suffice to identify the parameters controlling the particle distribution and block copolymer self-assembly. However, the more interesting and practically important case is one where the nanoparticles contain grafted polymers. As mentioned above, Kim and Matsen[162] recently presented an analysis of such a single particle case to deduce the distribution of such nanoparticles in the block copolymer phases. In earlier studies, Balazs and coworkers[172] considered the case of nondilute concentrations of particles but each containing just one grafted polymer (referred to as a "tadpole" configuration). They extended their density functional theories to address the self-assembly in such cases. In other research, Reister and Fredrickson[173] used a creative idea of modeling the grafted nanoparticle as a star polymer with a finite sized (soft) core to shed light on the self-assembly behavior one might expect. While these preceding studies and their results have been invaluable, issues such as the role of the molecular weight of the grafted polymer (relative to the matrix molecular weight), the grafting density of the nanoparticles and enthalpic interactions (if any) between the matrix polymer and the functionalizers are still unresolved and are expected to constitute active directions for future theoretical research.

V. Concluding remarks

In summary, we briefly reviewed some of the recent theoretical developments in the context of coarse-grained modeling of *equilibrium* characteristics of particle dispersion in homopolymer and block copolymer matrices. The studies reviewed were connected thematically by pointing out that in each of the instances, knowledge of particle–polymer interactions at the single particle level may not alone suffice to explain the dispersion and organization characteristics of the nanoparticles. In each case, we highlighted our contributions to the specific problem at hand and mentioned some related theoretical research and future directions. Admittedly, our perspective was biased, not only in the topics reviewed but also in the emphasis on certain class of modeling approaches.

We note that our discussions exclusively focused on theoretical descriptions of the "equilibrium" characteristics of particle

 This journal is © The Royal Society of Chemistry 2010

View Article Online

Published on 12 May 2010. Downloaded by University of Texas Libraries on 16/08/2013 15:20:49.

dispersion and assembly. However, despite the best experimental strategies, nonequilibrium effects resulting from spin casting, filler aggregation and/or external fields are bound to remain important for many applications of PNCs.[116,174] In this regard, many unresolved theoretical questions still remain: "how does the structure of a PNC dispersion evolve upon dispersing the fillers in the polymer matrix?", "can quantities such as the cluster size distributions and fractal dimensions be predicted for specified polymer-filler combinations?", "how does externally applied shear, electric and magnetic fields (and combinations thereof) impact upon the nonequilibrium state of the dispersion?"[32,175] While traditional computer simulations may shed light on some of the relevant issues pertaining to these questions, the time and length scales which can be probed by such means may not necessarily overlap with experimental regimes, and there is a need for development of new approaches to address the pertinent issues.

We emphasize that coarse-grained modeling is but one rung in the ladder of modeling approaches for materials structure and properties. Other approaches such as quantum mechanical calculations, atomistic simulations, integral equation theories and continuum mechanical approaches provide complementary information to effect predictive computer modeling of the structure and properties of materials. This complementarity becomes most evident when one desires to relate the parameters accompanying coarse-grained models to the chemical details of the polymer molecules and the filler. This requires the development of efficient multiscale computer simulation tools and methodologies which can render quantitatively the connection between the chemistry of the components, their force fields and the coarse-grained parameters.[34,35,49,51,176,177] Availability of such a suite of tools will render the *ab initio* computer-aided predictive characterization of properties of PNCs a reality.

Acknowledgements

VG's research program on polymer nanocomposites has been graciously supported by research grants from the Divisions of Materials Research (DMR) and Chemical and Biological Environmental and Transport Systems (CBET) of National Science Foundation. VG also acknowledges financial support from the American Chemical Society through their Petroleum Research Fund, Air Force Office For Scientific Research (through the CONTACT program), the Robert A. Welch Foundation (Grant F1599) and the US Army Research Office under grant W911NF-07-1-0268. CJE acknowledges financial support from the Robert A. Welch Foundation (Grant F-1709) and the American Chemical Society through their Petroleum Research Fund. VG also acknowledges Prof. Glenn Fredrickson, Edward Kramer, Frank Bates, Michael Rubinstein, Lynden Archer, Kenneth Schweizer, John Torkelson, Peter Green, Donald Paul, Jack Douglas, Sanat Kumar, Richard Vaia and Ramanan Krishnamoorti for many discussions and insights pertaining to polymer physics and polymer nanocomposites.

References

1 S. Torquato, *Random Heterogeneous Materials: Microstructure and Macroscopic Properties*, Springer, New York, 2002.
2 E. P. Giannelis, *Adv. Mater.*, 1996, **8**, 29.
3 E. P. Giannelis, R. Krishnamoorti and E. Manias, *Adv. Polym. Sci.*, 1999, **138**, 107–147.
4 M. Alexandre and P. Dubois, *Mater. Sci. Eng., R*, 2000, **28**, 1–63.
5 R. Andrews and M. C. Weisenberger, *Curr. Opin. Solid State Mater. Sci.*, 2004, **8**, 31–37.
6 E. T. Thostenson, C. Y. Li and T. W. Chou, *Compos. Sci. Technol.*, 2005, **65**, 491–516.
7 M. R. Bockstaller, R. A. Mickiewicz and E. L. Thomas, *Adv. Mater.*, 2005, **17**, 1331–1349.
8 A. C. Balazs, T. Emrick and T. P. Russell, *Science*, 2006, **314**, 1107–1110.
9 M. Moniruzzaman and K. I. Winey, *Macromolecules*, 2006, **39**, 5194–5205.
10 R. Krishnamoorti and R. A. Vaia, *J. Polym. Sci., Part B: Polym. Phys.*, 2007, **45**, 3252–3256.
11 S. S. Ray and M. Okamoto, *Prog. Polym. Sci.*, 2003, **28**, 1539–1641.
12 R. Krishnamoorti and K. Yurekli, *Curr. Opin. Colloid Interface Sci.*, 2001, **6**, 464–470.
13 R. E. Gorga and R. E. Cohen, *J. Polym. Sci., Part B: Polym. Phys.*, 2004, **42**, 2690–2702.
14 T. D. Fornes, P. J. Yoon, H. Keskkula and D. R. Paul, *Polymer*, 2001, **42**, 9929–9940.
15 S. Takahashi, H. A. Goldberg, C. A. Feeney, D. P. Karim, M. Farrell, K. O'Leary and D. R. Paul, *Polymer*, 2006, **47**, 3083–3093.
16 J. W. Gilman, T. Kashiwagi and J. D. Lichtenhan, *SAMPE J.*, 1997, **33**, 40–46.
17 D. Porter, E. Metcalfe and M. J. K. Thomas, *Fire Mater.*, 2000, **24**, 45–52.
18 L. L. Beecroft and C. K. Ober, *Chem. Mater.*, 1997, **9**, 1302–1317.
19 W. Caseri, *Macromol. Rapid Commun.*, 2000, **21**, 705–722.
20 D. Y. Godovski, *Adv. Polym. Sci.*, 1995, **119**, 79–122.
21 G. Brusatin and R. Signorini, *J. Mater. Chem.*, 2002, **12**, 1964–1977.
22 F. M. Du, J. E. Fischer and K. I. Winey, *Phys. Rev. B: Condens. Matter Mater. Phys.*, 2005, **72**, 121404.
23 J. Pyun, *Polym. Rev.*, 2007, **47**, 231–263.
24 J. Oberdisse, *Soft Matter*, 2006, **2**, 29–36.
25 N. Grossiord, J. Loos, O. Regev and C. E. Koning, *Chem. Mater.*, 2006, **18**, 1089–1099.
26 J. Hilding, E. A. Grulke, Z. G. Zhang and F. Lockwood, *J. Dispersion Sci. Technol.*, 2003, **24**, 1–41.
27 J. M. Kropka, K. W. Putz, V. Pryamitsyn, V. Ganesan and P. F. Green, *Macromolecules*, 2007, **40**, 5424–5432.
28 L. Khounlavong and V. Ganesan, *J. Chem. Phys.*, 2009, **130**, 104901.
29 V. Ganesan, L. Khounlavong and V. Pryamitsyn, *Phys. Rev. E: Stat., Nonlinear, Soft Matter Phys.*, 2008, **78**, 051804.
30 T. D. Fornes, D. L. Hunter and D. R. Paul, *Macromolecules*, 2004, **37**, 1793–1798.
31 M. Z. Rong, M. Q. Zhang, Y. X. Zheng, H. M. Zeng, R. Walter and K. Friedrich, *Polymer*, 2001, **42**, 167–183.
32 J. Masuda and J. M. Torkelson, *Macromolecules*, 2008, **41**, 5974–5977.
33 D. Bedrov, G. D. Smith and J. S. Smith, *J. Chem. Phys.*, 2003, **119**, 10438–10447.
34 N. Sheng, M. C. Boyce, D. M. Parks, G. C. Rutledge, J. I. Abes and R. E. Cohen, *Polymer*, 2004, **45**, 487–506.
35 O. Borodin, D. Bedrov, G. D. Smith, J. Nairn and S. Bardenhagen, *J. Polym. Sci., Part B: Polym. Phys.*, 2005, **43**, 1005–1013.
36 L. M. Hall, A. Jayaraman and K. S. Schweizer, *Curr. Opin. Solid State Mater. Sci.*, 2010, **14**(8), 38–48.
37 J. Huh, V. V. Ginzburg and A. C. Balazs, *Macromolecules*, 2000, **33**, 8085–8096.
38 S. W. Sides, B. J. Kim, E. J. Kramer and G. H. Fredrickson, *Phys. Rev. Lett.*, 2006, **96**, 250601.
39 M. Surve, V. Pryamitsyn and V. Ganesan, *J. Chem. Phys.*, 2005, **122**, 154901.
40 V. Pryamitsyn and V. Ganesan, *J. Chem. Phys.*, 2005, **122**, 104906.
41 M. Surve, V. Pryamitsyn and V. Ganesan, *J. Chem. Phys.*, 2006, **125**, 064903.
42 V. Pryamitsyn and V. Ganesan, *Macromolecules*, 2006, **39**, 8499–8510.
43 M. Surve, V. Pryamitsyn and V. Ganesan, *Phys. Rev. Lett.*, 2006, **96**, 177805.
44 M. Surve, V. Pryamitsyn and V. Ganesan, *Langmuir*, 2006, **22**, 969–981.

View Article Online

Published on 12 May 2010. Downloaded by University of Texas Libraries on 16/08/2013 15:20:49.

45 V. Pryamitsyn and V. Ganesan, *Macromolecules*, 2006, **39**, 844–856.
46 V. Pryamitsyn and V. Ganesan, *J. Rheol.*, 2006, **50**, 655–683.
47 M. Surve, V. Pryamitsyn and V. Ganesan, *Macromolecules*, 2007, **40**, 344–354.
48 J. Baschnagel, K. Binder, P. Doruker, A. A. Gusev, O. Hahn, K. Kremer, W. L. Mattice, F. Muller-Plathe, M. Murat, W. Paul, S. Santos, U. W. Suter and V. Tries, Advances in polymer science: viscoelasticity, atomistic models, *Stat. Chem.*, 2000, **152**, 41–156.
49 F. Muller-Plathe, *ChemPhysChem*, 2002, **3**, 754–769.
50 G. H. Fredrickson, *The Equilibrium Theory of Inhomogeneous Polymers*, Clarendon Press, Oxford, New York, 2006.
51 J. J. de Pablo and W. A. Curtin, *MRS Bull.*, 2007, **32**, 905–911.
52 D. Q. Pike, F. A. Detcheverry, M. Muller and J. J. de Pablo, *J. Chem. Phys.*, 2009, **131**, 084903.
53 J. B. Hooper and K. S. Schweizer, *Macromolecules*, 2007, **40**, 6998–7008.
54 G. H. Fredrickson, V. Ganesan and F. Drolet, *Macromolecules*, 2002, **35**, 16–39.
55 M. Dijkstra, R. van Roij and R. Evans, *Phys. Rev. Lett.*, 1998, **81**, 2268–2271.
56 M. Dijkstra, R. van Roij and R. Evans, *Phys. Rev. E: Stat. Phys., Plasmas, Fluids, Relat. Interdiscip. Top.*, 1999, **59**, 5744–5771.
57 M. Doi and S. Edwards, *The Theory of Polymer Dynamics*, Oxford University Press/Clarendon Press, Oxford, New York, 1986.
58 P. G. De Gennes, *Macromolecules*, 1982, **15**, 492–500.
59 P. G. De Gennes, *Macromolecules*, 1981, **14**, 1637–1644.
60 J. R. Roan and T. Kawakatsu, *J. Chem. Phys.*, 2002, **116**, 7283–7294.
61 J. F. Joanny, L. Leibler and P. G. De Gennes, *J. Polym. Sci., Part B: Polym. Phys.*, 1979, **17**, 1073–1084.
62 T. Odijk, *Langmuir*, 1997, **13**, 3579–3581.
63 T. Odijk, *J. Chem. Phys.*, 1997, **106**, 3402–3406.
64 I. Lynch, S. Cornen and L. Piculell, *J. Phys. Chem. B*, 2004, **108**, 5443–5452.
65 G. J. Fleer, A. M. Skvortsov and R. Tuinier, *Macromolecules*, 2003, **36**, 7857–7872.
66 H. N. W. Lekkerkerker, W. C. K. Poon, P. N. Pusey, A. Stroobants and P. B. Warren, *Europhys. Lett.*, 1992, **20**, 559–564.
67 C. Cabane, K. Wong and R. Duplessix, *ACS Symp. Ser.*, 1989, **384**, 312–327.
68 E. Dickinson, *Colloids Surf., B*, 2001, **20**, 197–210.
69 Y. Otsubo and Y. Nakane, *Langmuir*, 1991, **7**, 1118–1123.
70 H. Ji, D. Hone, P. A. Pincus and G. Rossi, *Macromolecules*, 1990, **23**, 698–707.
71 P. J. Flory and G. Ronca, *Mol. Cryst. Liq. Cryst.*, 1979, **54**, 289–309.
72 P. J. Flory and G. Ronca, *Mol. Cryst. Liq. Cryst.*, 1979, **54**, 311–330.
73 S. Asakura and F. Oosawa, *J. Polym. Sci.*, 1958, **33**, 183.
74 A. Vrij, *Pure Appl. Chem.*, 1976, **48**, 471.
75 E. J. Meijer and D. Frenkel, *Phys. Rev. Lett.*, 1991, **67**, 1110–1113.
76 A. P. Chatterjee and K. S. Schweizer, *J. Chem. Phys.*, 1998, **109**, 10464–10476.
77 Y. L. Chen, K. S. Schweizer and M. Fuchs, *J. Chem. Phys.*, 2003, **118**, 3880–3890.
78 M. Fuchs and K. S. Schweizer, *Europhys. Lett.*, 2000, **51**, 621–627.
79 S. Ramakrishnan, M. Fuchs, K. S. Schweizer and C. F. Zukoski, *Langmuir*, 2002, **18**, 1082–1090.
80 S. Ramakrishnan, M. Fuchs, K. S. Schweizer and C. F. Zukoski, *J. Chem. Phys.*, 2002, **116**, 2201–2212.
81 M. Fuchs and K. S. Schweizer, *J. Phys.: Condens. Matter*, 2002, **14**, R239–R269.
82 P. G. Bolhuis, A. A. Louis and J. P. Hansen, *Phys. Rev. Lett.*, 2002, **89**, 128302.
83 P. G. Bolhuis, E. J. Meijer and A. A. Louis, *Phys. Rev. Lett.*, 2003, **90**, 068304.
84 D. G. A. L. Aarts, R. Tuinier and H. N. W. Lekkerkerker, *J. Phys.: Condens. Matter*, 2002, **14**, 7551–7561.
85 R. Tuinier and A. V. Petukhov, *Macromol. Theory Simul.*, 2002, **11**, 975–984.
86 R. Tuinier, D. G. A. L. Aarts, H. H. Wensink and H. N. W. Lekkerkerker, *Phys. Chem. Chem. Phys.*, 2003, **5**, 3707–3715.
87 R. Tuinier, J. Rieger and C. G. de Kruif, *Adv. Colloid Interface Sci.*, 2003, **103**, 1–31.
88 P. Paricaud, S. Varga and G. Jackson, *J. Chem. Phys.*, 2003, **118**, 8525–8536.
89 H. M. Schaink and J. A. M. Smit, *J. Chem. Phys.*, 1997, **107**, 1004–1015.
90 A. N. Semenov, J. B. Avalos, A. Johner and J. F. Joanny, *Macromolecules*, 1996, **29**, 2179–2196.
91 M. Aubouy, O. Guiselin and E. Raphael, *Macromolecules*, 1996, **29**, 7261–7268.
92 A. Yethiraj and C. E. Woodward, *J. Chem. Phys.*, 1995, **102**, 5499–5505.
93 A. Yethiraj, *Chem. Eng. J.*, 1999, **74**, 109–115.
94 P. A. Pincus, C. J. Sandroff and T. A. Witten, *J. Phys.*, 1984, **45**, 725–729.
95 M. Aubouy, J. M. Dimeglio and E. Raphael, *Europhys. Lett.*, 1993, **24**, 87–92.
96 R. A. Vaia and E. P. Giannelis, *Macromolecules*, 1997, **30**, 8000–8009.
97 A. C. Balazs, C. Singh and E. Zhulina, *Macromolecules*, 1998, **31**, 8370–8381.
98 V. V. Ginzburg and A. C. Balazs, *Macromolecules*, 1999, **32**, 5681–5688.
99 V. V. Ginzburg, C. Singh and A. C. Balazs, *Macromolecules*, 2000, **33**, 1089–1099.
100 L. M. Hall and K. S. Schweizer, *J. Chem. Phys.*, 2008, **128**, 234901.
101 J. B. Hooper and K. S. Schweizer, *Macromolecules*, 2006, **39**, 5133–5142.
102 R. Dickman and A. Yethiraj, *J. Chem. Phys.*, 1994, **100**, 4683–4690.
103 M. Vacatello, *Macromol. Theory Simul.*, 2002, **11**, 757–765.
104 D. Brown, P. Mele, S. Marceau and N. D. Alberola, *Macromolecules*, 2003, **36**, 1395–1406.
105 A. Striolo, C. M. Colina, K. E. Gubbins, N. Elvassore and L. Lue, *Mol. Simul.*, 2004, **30**, 437–449.
106 J. B. Hooper, K. S. Schweizer, T. G. Desai, R. Koshy and P. Keblinski, *J. Chem. Phys.*, 2004, **121**, 6986–6997.
107 H. Lin, F. Erguney and W. L. Mattice, *Polymer*, 2005, **46**, 6154–6162.
108 P. J. Dionne, C. R. Picu and R. Ozisik, *Macromolecules*, 2006, **39**, 3089–3092.
109 J. H. Huang, Z. F. Mao and C. J. Qian, *Polymer*, 2006, **47**, 2928–2932.
110 G. Allegra, G. Raos and M. Vacatello, *Prog. Polym. Sci.*, 2008, **33**, 683–731.
111 M. Doxastakis, Y. L. Chen, O. Guzman and J. J. de Pablo, *J. Chem. Phys.*, 2004, **120**, 9335–9342.
112 O. Guzman and J. J. de Pablo, *J. Chem. Phys.*, 2003, **118**, 2392–2397.
113 J. E. Riggs, D. B. Walker, D. L. Carroll and Y. P. Sun, *J. Phys. Chem. B*, 2000, **104**, 7071–7076.
114 R. Hasegawa, Y. Aoki and M. Doi, *Macromolecules*, 1996, **29**, 6656–6662.
115 A. Bansal, H. C. Yang, C. Z. Li, R. C. Benicewicz, S. K. Kumar and L. S. Schadler, *J. Polym. Sci., Part B: Polym. Phys.*, 2006, **44**, 2944–2950.
116 L. Meli and P. F. Green, *ACS Nano*, 2008, **2**, 1305–1312.
117 P. K. Sudeep, Z. Page and T. Emrick, *Chem. Commun.*, 2008, 6126–6127.
118 L. Leibler and A. Mourran, *MRS Bull.*, 1997, **22**, 33–37.
119 P. G. Ferreira, A. Ajdari and L. Leibler, *Macromolecules*, 1998, **31**, 3994–4003.
120 M. W. Matsen and J. M. Gardiner, *J. Chem. Phys.*, 2001, **115**, 2794–2804.
121 A. P. Gast and L. Leibler, *Macromolecules*, 1986, **19**, 686–691.
122 D. L. Green and J. Mewis, *Langmuir*, 2006, **22**, 9546–9553.
123 X. R. Wang, V. J. Foltz, M. Rackaitis and G. G. A. Bohm, *Polymer*, 2008, **49**, 5683–5691.
124 N. Dutta and D. Green, *Langmuir*, 2008, **24**, 5260–5269.
125 A. Striolo and S. A. Egorov, *J. Chem. Phys.*, 2007, **126**, 014902.
126 S. Jain, V. V. Ginzburg, P. Jog, J. Weinhold, R. Srivastava and W. G. Chapman, *J. Chem. Phys.*, 2009, **131**, 044908.
127 C. M. Wijmans, F. A. M. Leermakers and G. J. Fleer, *Langmuir*, 1994, **10**, 4514–4516.
128 J. U. Kim and M. W. Matsen, *Macromolecules*, 2008, **41**, 4435–4443.
129 E. Lindberg and C. Elvingson, *J. Chem. Phys.*, 2001, **114**, 6343–6352.
130 K. T. Marla and J. C. Meredith, *J. Chem. Theory Comput.*, 2006, **2**, 1624–1631.
131 D. Duque, B. K. Peterson and L. F. Vega, *J. Phys. Chem. C*, 2007, **111**, 12328–12334.
132 G. D. Smith and D. Bedrov, *Langmuir*, 2009, **25**, 11239–11243.

 This journal is © The Royal Society of Chemistry 2010

View Article Online

133 S. A. Egorov, *J. Chem. Phys.*, 2008, **129**, 064901.
134 J. J. Xu, F. Qiu, H. D. Zhang and Y. L. Yang, *J. Polym. Sci., Part B: Polym. Phys.*, 2006, **44**, 2811–2820.
135 S. E. Harton and S. K. Kumar, *J. Polym. Sci., Part B: Polym. Phys.*, 2008, **46**, 351–358.
136 A. Jayaraman and K. S. Schweizer, *Macromolecules*, 2008, **41**, 9430–9438.
137 A. Jayaraman and K. S. Schweizer, *Langmuir*, 2008, **24**, 11119–11130.
138 A. Jayaraman and K. S. Schweizer, *Mol. Simul.*, 2009, **35**, 835–848.
139 A. Jayaraman and K. S. Schweizer, *Macromolecules*, 2009, **42**, 8423–8434.
140 I. Borukhov and L. Leibler, *Phys. Rev. E: Stat. Phys., Plasmas, Fluids, Relat. Interdiscip. Top.*, 2000, **62**, R41–R44.
141 I. Borukhov and L. Leibler, *Macromolecules*, 2002, **35**, 5171–5182.
142 B. Kim, D. Y. Ryu, V. Pryamitsyn and V. Ganesan, *Macromolecules*, 2009, **42**, 7919–7923.
143 P. Akcora, H. Liu, S. K. Kumar, J. Moll, Y. Li, B. C. Benicewicz, L. S. Schadler, D. Acehan, A. Z. Panagiotopoulos, V. Pryamitsyn, V. Ganesan, J. Ilavsky, P. Thiyagarajan, R. H. Colby and J. F. Douglas, *Nat. Mater.*, 2009, **8**, 354–U121.
144 V. Pryamtisyn, V. Ganesan, A. Z. Panagiotopoulos, H. Liu and S. K. Kumar, *J. Chem. Phys.*, 2009, **131**, 221102.
145 M. R. Bockstaller, Y. Lapetnikov, S. Margel and E. L. Thomas, *J. Am. Chem. Soc.*, 2003, **125**, 5276–5277.
146 A. Haryono and W. H. Binder, *Small*, 2006, **2**, 600–611.
147 J. J. Chiu, B. J. Kim, E. J. Kramer and D. J. Pine, *J. Am. Chem. Soc.*, 2005, **127**, 5036–5037.
148 V. J. Leppert, A. K. Murali, S. H. Risbud, M. Stender, P. P. Power, C. Nelson, P. Banerjee and A. M. Mayes, *Philos. Mag. B*, 2002, **82**, 1047–1054.
149 V. Lauter-Pasyuk, H. J. Lauter, G. P. Gordeev, P. Muller-Buschbaum, B. P. Toperverg, M. Jernenkov and W. Petry, *Langmuir*, 2003, **19**, 7783–7788.
150 J. J. Chiu, B. J. Kim, G. R. Yi, J. Bang, E. J. Kramer and D. J. Pine, *Macromolecules*, 2007, **40**, 3361–3365.
151 A. Jain, J. S. Gutmann, C. B. W. Garcia, Y. M. Zhang, M. W. Tate, S. M. Gruner and U. Wiesner, *Macromolecules*, 2002, **35**, 4862–4865.
152 M. R. Bockstaller and E. L. Thomas, *Phys. Rev. Lett.*, 2004, **93**, 166106.
153 S. C. Warren, L. C. Messina, L. S. Slaughter, M. Kamperman, Q. Zhou, S. M. Gruner, F. J. DiSalvo and U. Wiesner, *Science*, 2008, **320**, 1748–1752.
154 B. J. Kim, G. H. Fredrickson, C. J. Hawker and E. J. Kramer, *Langmuir*, 2007, **23**, 7804–7809.
155 M. K. Gaines, S. D. Smith, J. Samseth, M. R. Bockstaller, R. B. Thompson, K. O. Rasmussen and R. J. Spontak, *Soft Matter*, 2008, **4**, 1609–1612.
156 A. J. Schultz, C. K. Hall and J. Genzer, *Macromolecules*, 2005, **38**, 3007–3016.
157 W. A. Lopes, *Phys. Rev. E: Stat., Nonlinear, Soft Matter Phys.*, 2002, **65**, 031606.
158 D. R. M. Williams and P. A. Pincus, *Europhys. Lett.*, 1993, **24**, 29–34.
159 J. U. Kim and B. O'Shaughnessy, *Macromolecules*, 2006, **39**, 413–425.
160 M. W. Matsen and R. B. Thompson, *Macromolecules*, 2008, **41**, 1853–1860.
161 J. U. Kim and M. W. Matsen, *Macromolecules*, 2008, **41**, 246–252.
162 J. U. Kim and M. W. Matsen, *Phys. Rev. Lett.*, 2009, **102**, 078303.
163 V. V. Ginzburg, C. Gibbons, F. Qiu, G. W. Peng and A. C. Balazs, *Macromolecules*, 2000, **33**, 6140–6147.
164 R. B. Thompson, V. V. Ginzburg, M. W. Matsen and A. C. Balazs, *Science*, 2001, **292**, 2469–2472.
165 R. B. Thompson, V. V. Ginzburg, M. W. Matsen and A. C. Balazs, *Macromolecules*, 2002, **35**, 1060–1071.
166 A. I. Chervanyov and A. C. Balazs, *J. Chem. Phys.*, 2003, **119**, 3529–3534.
167 L. L. He, L. X. Zhang and H. J. Liang, *J. Phys. Chem. B*, 2008, **112**, 4194–4203.
168 F. D. A. A. Reis, *Macromolecules*, 2008, **41**, 8932–8937.
169 J. Z. Jin, J. Z. Wu and A. L. Frischknecht, *Macromolecules*, 2009, **42**, 7537–7544.
170 F. A. Detcheverry, H. M. Kang, K. C. Daoulas, M. Muller, P. F. Nealey and J. J. de Pablo, *Macromolecules*, 2008, **41**, 4989–5001.
171 F. A. Detcheverry, D. Q. Pike, P. F. Nealey, M. Muller and J. J. de Pablo, *Phys. Rev. Lett.*, 2009, **102**, 197801.
172 J. Y. Lee, A. C. Balazs, R. B. Thompson and R. M. Hill, *Macromolecules*, 2004, **37**, 3536–3539.
173 E. Reister and G. H. Fredrickson, *J. Chem. Phys.*, 2005, **123**, 214903.
174 J. B. He, R. Tangirala, T. Emrick, T. P. Russell, A. Boker, X. F. Li and J. Wang, *Adv. Mater.*, 2007, **19**, 381.
175 V. Pryamitsyn and V. Ganesan, *Macromolecules*, 2009, **42**, 7184–7193.
176 Q. H. Zeng, A. B. Yu and G. Q. Lu, *Prog. Polym. Sci.*, 2008, **33**, 191–269.
177 J. Bicerano, S. Balijepalli, A. Doufas, V. Ginzburg, J. Moore, M. Somasi, S. Somasi, J. Storer and T. Verbrugge, *J. Macromol. Sci., Polym. Rev.*, 2004, **C44**, 53–85.

Published on 12 May 2010. Downloaded by University of Texas Libraries on 16/08/2013 15:20:49.